PREPRINT UCRL-78379

Lawrence Livermore Laboratory

Quantum Statistical Models for Multicomponent Plasmas

Balazs F. Rozsnyai and Berni J. Alder

June 1976

This paper was prepared for submission to Phys. Rev. A.

QUANTUM STATISTICAL MODELS FOR MULTICOMPONENT PLASMAS*

Balazs F. Rozsnyai and Berni J. Alder

Lawrence Livermore Laboratory, University of Calfornia

Livermore, California 94550

Abstract

The Thomas-Fermi-Dirac theory and one that adds Debye-Hückel interaction between particles is described for mixtures. The differences in the predictions of the two models are evaluated for the mixtures of iron and hydrogen under astrophysical conditions.

1. Introduction

The temperature and density-dependent Thomas-Fermi and Thomas-Fermi-Dirac theories for one component matter were developed some time ago.[1,2] In these theories the state of the matter is represented by the state of an atom enclosed in a sphere whose radius is determined by the matter density. The charge neutrality requires that each spherical volume contains Z statistically distributed electrons, where Z is the nuclear charge. Since each sphere is neutral, interactions between neighboring atoms are neglected. This model was improved to include shell effects,[3] and subsequently, it was developed to a self-consistent Hartree-Slater "average atom" model.[4]

---

*Work performed under the auspices of the U.S. Energy Research and Development Administration contract No. W-7405-Eng-48.

A statistical model, which accounts for the interaction between neighbors in the low density limit by permitting the charge densities to diffuse into each others neighborhood, was described by Cowan and Kirkwood,[5] and was called the Debye-Hückel, Thomas-Fermi (DHTF) theory.

The purpose of this report is to extend these two statistical models to multicomponent Z matter and to compare some of the predictions of the two theories. Accordingly, two models are discussed, the "confined atom Thomas-Fermi-Dirac" (CATFD) model and the "Debye-Hückel Thomas-Fermi-Dirac" (DHTFD) model. In both models the effect of exchange and correlation is taken into account by a localized exchange and correlation potential in an approximation described in Ref. 4. Unless stated otherwise, all quantities are computed in atomic units.

2. Theory

A. The CATFD Model

In the CATFD model each atom is enclosed in a spherical volume which contains Z_i electrons (bound and free) where Z_i is the nuclear charge. For a one-component system the radius of each cell is the same, $R = (3M/4\pi\rho)^{1/3}$, where ρ is the matter density (g/cm^3) and M is the mass of the atom. For a mixture the radius R_i for an atom with nuclear charge Z_i and mass M_i is determined by the condition that the chemical potential or Fermi level of the electrons has to be the same for each cell at a given temperature and density. This

necessarily implies that the electron pressure is also the same in each cell. However, the pressure due to the nuclei in each cell are not the same and the nuclear pressure must be computed for the system as a whole. The single radius in the mixture is replaced by a mean radius defined by

$$\bar{R} = (3\bar{M}/n\pi\rho)^{1/3} , \tag{1}$$

where

$$M = \Sigma x_i M_i$$

and x_i and M_i are the mole fraction and atomic mass of the i*th* component, respectively. The component R_i-s and $\bar{R}$ are connected by the volume normalization

$$\Sigma x_i R_i^3 = \bar{R}^3 \tag{2}$$

For each component the electron density is given by

$$\rho_i^e(r) = A\, I_{1/2}\{[\mu - V_i(r)]/kT\} , \tag{3}$$

where $A = \frac{4\pi}{h^3}[2mkT]^{3/2}$, kT is the temperature in energy units, m is the electron mass, r denotes the distance from the nucleus, μ is the chemical potential, $V_i(r)$ is the electron potential for the component i and I is the Fermi-Dirac integral given by

$$I_\nu(x) = \int_0^\infty \frac{t^\nu}{e^{t-x} + 1}\, dt . \tag{4}$$

The electron potential is given by

$$V_i(r) = - Z_i/r + V_i^{ee}(r) + V_i^{ex}(r) + V_i^{corr}(r), \qquad (5)$$

where V_i^{ex} and V_i^{corr} are the contributions from the exchange and correlation as described in Ref. 4 and the classical electron- electron interaction is given by

$$V_i^{ee}(r) = 4\pi\left[\frac{1}{r}\int_o^r \rho_i^e(r')r'^2\ dr' + \int_r^{R_i} \rho_i^e(r')r'dr'\right]. \qquad (6)$$

Equations (1)-(6) form the complete self-consistent set of equations of the CATFD model and within the validity of that model they determine the state of the matter. It should be noted that in addition to μ, the other quantities which are characteristic of the state of the matter are the potential and electron density at the boundary of any cell which have to match,

$$V_i(R_i) = V_j(R_j) = V_f;\ \rho_i^e(R_i) = \rho_j^e(R_j) = \rho_f$$

where V_f and ρ_f can be regarded as the free electron potential and density, respectively. Some other relevant quantities are

$$Z_i^* = \frac{4\pi}{3} R_i^3 \rho_f = \text{effective nuclear charge}, \qquad (7)$$

the electron pressure

$$P_e = \frac{2}{3} A\ kTI_{3/2}\left\{[\mu - V_f]/kT\right\} \qquad (8)$$

and the nuclear pressure

$$P_N = \frac{3kT}{4\pi\bar{R}^3} \qquad (9)$$

which assumes that the nuclei can be treated as a perfect gas. The electronic energy for the i*th* component is given by

$$E_i = E_{kin,i} + E_{eN,i} + E_{ee,i}$$

where the three terms stand for the kinetic, electron-nuclear and electron-electron energies given by

$$E_{kin,i} = 4\pi AkT \int_o^{R_i} I_{3/2}\{[\mu - V_i(r)]/kT\}\, r^2\, dr \tag{11}$$

$$E_{eN,i} = -\, Z_i 4\pi \int_o^{R_i} \rho_i{}^e(r) r\, dr \tag{12}$$

$$E_{ee,i} = 2\pi \int_o^{R_i} V_i{}^{ee}(r)\, \rho_i{}^e(r)\, r^2\, dr\ . \tag{13}$$

The electron entropy for the i*th* component is given by (see Ref. 2)

$$TS_i = \frac{5}{3} E_{kin,i} + E_{eN,i} + 2E_{ee,i} - \mu Z_i \tag{14}$$

For a mixture the relevant quantities are the total energy and entropy for a spherical volume with the mean radius $\bar{R}$

$$E = \Sigma x_i E_i + \frac{3}{2} kT \tag{15}$$

$$TS = T\, \Sigma x_i S_i + 3kT\, \Sigma x_i \ln \frac{\bar{R}}{R_i{}^o}\ , \tag{16}$$

where the last term in Eq. (15) is the contribution of the nuclear kinetic energy and the last term in Eq. (16) is the contribution to

the entropy due to the mixing of atoms and R_i^o is the radius of the one component matter under the same condition (temperature, volume or pressure) as the mixture. Equations (8)-(16) provide the basis for the calculation of the thermodynamic potentials in the CATFD approximation.

B. The DHTFD Model

In the DHTFD model each componetn is considered as a test particle with $R_i \sim \infty$. The electron distribution around the nuclear charge Z_i is given by Eq. (3) as in the CATFD model. In addition, the rest of the positively charged ions are distributed according to the Baltzmann statistics

$$\rho_i^+ (r) = \rho_i^{+0} \{\exp \bar{Z} [V_i(r) - V_i(\infty)]/kT\} \tag{17}$$

where $\bar{Z}$ is the average effective nuclear charge given by

$$\bar{Z} = \Sigma\ x_i\ Z_i^* \tag{18}$$

The electron potential is given by

$$V_i(r) = -Z_i/r + V_i^{ee}(r) + V_i^{ex}(r) + V_i^{corr}(r) + V_i^{e+}(r), \tag{19}$$

where the first four terms are the same as in Eq. (5) and the last term is due to the positive charge distribution. The combined formula for V_i^{ee} and V_i^{e+} is given by

$$V_i^{ee}(r) + V_i^{e+}(r) = 4\pi\left\{\frac{1}{r}\int_o^r \left[\rho_i^{ee}(r') - \rho_i^{e+}(r')\right] r'^2\, dr + \int^{\infty} [\rho_i^{ee}(r') - \rho_i^{e+}(r')] r'\, dr'\right\} . \tag{20}$$

Charge neutrality conditions require that

$$\rho_i^{+o} = \rho^{+o} = \rho_f \text{ independent of } i,$$

$$V_i(r) \to V_f \text{ as } \to \infty \qquad \text{independent of } i$$

which also assures that the integral in Eq. (20) does not become divergent.

It should be observed that although in the DHTFD model the individual values of R_{i-s} lose their meaning, the mean radius $\bar{R}$ remains a well-defined quantity, determined solely by the atomic masses, mole fractions and the matter density. In the DHTFD model the quantity analogous to R_i of the CATFD model can be defined as the "radius of neutrality" given by

$$\int_o^{R_i'} \rho_i^e(r)\, r^2\, dr = Z_i \tag{21}$$

Since the charge distributions in the two models are different; the values of R_i and R_i' are different as well. The effective nuclear charges are given by Eq. (7) with R_i' replacing R_i. The charge neutrality condition requires that

$$\rho^{+o} = \rho_f = \frac{3}{4\pi} \frac{\bar{Z}}{\bar{R}^3} \tag{22}$$

3. Calculations

Iron and hydrogen mixture was selected as an example. This mixture if of astrophysical interest, and, with the appearance of high powered lasers, the region of high pressure and temperature has also become

of interest in laser-fusion research. Some of the data are summarized in Tables I and II at temperature of 1 keV and a pressure of 10^5 Mbar; a condition which exist in the center region of the sun.[7] The symbol x stands for the mole fraction of iron and η is the chemical potential of the electrons divided by kT. Both the CATFD and DHTFD models yield the same η shown in the second column of Table I. The mean radii and atomic radii are shown in columns 3-7 of Table I. One can see that at the same temperature and pressure the DHTFD model predicts a small contraction compared to the CATFD model.

In Table II the electron potentials V_f and effective nuclear charges, as defined in the text, are given. The DHTFD model predicts somewhat smaller effective charges than the CATFD model. This is to be expected since more penetrating positive charge in the DHTFD model attracts more electrons. The considerable difference in V_{f-s} predicted by the two models is noteworthy. This difference is largest for pure hydrogen (x=0) and smallest for pure iron. It should be kept in mind that, although the chemical potentials are the same for the two models (up to four decimals), the degeneracy parameters for the free electrons are $\eta - V_f/kT$, which are hence different.

Some other comparisons are presented graphically. Figures 1 and 2 show the ratio of positive and negative charge densities given by the DHTFD model for hydrogen and iron, respectively. The temperature and pressure are again 1 keV and 10^5 Mbar, and the results for three values for the iron mole fraction are shown. The vertical bars

mark the position of R_i as predicted by the CATFD model. The CATFD model tacitly assures a step fraction for the ratio ρ^+/ρ^e. The differences in the electron potentials predicted by the two models are shown in Figs. 3-6. The quantity $r \times [V_i(r) - V_f]$ is plotted which has to be Z_i at $r = 0$. Again, the vertical marks indicate the position of R_i of the CATFD model. Figures 3 and 4 show the electron potentials for hydrogen and iron respectively, at 1 keV and 10^5 Mbar. Figures 5 and 6 show the same for 10 eV and 10^2 Mbar. This later condition is representative of the surface of a massive star, like a white dwarf.

It is interesting to investigate the effect of mixing on the Gibbs potential at constant temperature and pressure in order to establish possible phase separation. This was done only for the CATFD model and the results are shown in Figs. 7 and 8. The change in the Gibbs potential due to mixing is given by

$$\Delta G(x) = G(x) - X\, G_{Fe} - (1-x)\, G_{HY} , \qquad (23)$$

where $G(x)$ is the Gibbs function for the mixture and G_{Fe} and G_{HY} are the same for the pure compounds. Figure 7 shows ΔG as a function of the iron mole fraction x, at conditions which are near to that at the center of the sun. One can see that the mixing is always favorable. Figure 8 shows the same, at the relatively low temperature of 10 eV. At 10^2 Mbar, a condition which may exist in white dwarfs. the CATFD model clearly predicts phase separation. At 10 eV and 2 Mbar pressure the phase separation is no longer predicted. However, it should be

noted that at 10 eV and low pressure, the accuracy of any statistical model is questionable, because shell effects may be important.

The calculation of thermodynamic properties in the DHTFD model will be presented in a forthcoming paper.

Acknowledgment

The authors wish to thank Dr. E. L. Pollock for useful discussions during the course of this work.

References

1. R. P. Feynman, N. Metropolis and E. Teller, Phys. Rev. 75, 1561 (1969)
2. R. D. Cowan and J. Ashkin, Phys. Rev. 105, 144 (1957)
3. J. W. Zink, Phys. Rev. 176, 279 (1968)
4. B. F. Rozsnyai, Phys. Rev. 514, 1137 (1972)
5. R. D. Cowan and J. G. Kirkwood, J. Chem. Phys. 29, 264 (1958)
6. Equation (7) assumes that the free electron density is uniform. Detailed Hartree-Slater calcualtions of Ref. 4 confirm that this is a very good approximation.
7. See D. D. Clayton "Principles of Stellar Evolution and Nucleo-synthesis" McGraw-Hill 1968

Table I. Electron chemical potential and atomic radii for iron-hyrdrogen mixture at kT = 1 KeV P = 10^5 Mb.

X	η	$\bar{R}$		R_i(CATFD)		R_i'(DHTFD)	
		CATFD	DHTFO	R_{HY}	R_{Fe}	R'_{HY}	R'_{Fe}
0	-1.792	.3726	.3696	.3726	-	.3697	-
.1	-1.398	.4639	.4566	.3286	.8789	.3229	.8382
.2	-1.284	.5279	.5207	.3171	.8472	.3121	.8174
.3	-1.232	.5797	.5723	.3120	.8332	.3071	.8071
.4	-1.202	.6236	.6162	.3091	.8252	.3042	.8026
.5	-1.182	.6621	.6539	.3072	.8200	.3023	.8007
.6	-1.168	.6965	.6896	.3058	.8164	.3022	.8003
.8	-1.149	.7568	.7481	.3041	.8117	.3005	.7973
.9	-1.138	.7824	.7760	.3030	.8088	.2994	.7961
1.	-1.136	.8085	.8016	-	.8085	-	.7958

Table II. Electron potentials V_f and effective nuclear charges for iron-hydrogen mixture at kT = 1 KeV P = 10^5 Mb.

	V_f		Z_i^* (CATFD)		Z_i^* (DHTFD)		$\bar{Z}$	
X	CATFD	DHTFD	Z_{HY}^*	Z_{Fe}^*	Z_{HY}^*	Z_{Fe}^*	CATFD	DHTFD
0	-.4463	-1.580	.9774	-	.9541		.9774	.9541
.1	-.6468	-1.721	.9749	18.68	.9431	17.47	2.746	2.595
.2	-.7178	-1.542	.9742	18.61	.9445	17.60	4.501	4.276
.3	-.7568	-1.394	.9739	18.58	.9442	17.72	6.256	5.976
.4	-.7822	-1.295	.9737	18.56	.9438	17.80	8.010	7.687
.5	-.8011	-1.314	.9736	18.55	.9441	17.80	9.764	9.373
.6	-.8160	-1.238	.9735	18.55	.9538	17.94	11.52	11.14
.8	-.8394	-1.167	.9734	18.54	.9520	17.88	15.02	14.49
.9	-.8523	-1.111	.9734	18.53	.9527	18.06	16.78	16.35
1	-.8586	- .9476	-	18.53	-	18.03	18.53	18.03

Figure Captions

Fig. 1. Ratio of positive and negative charge densities in hydrogen for various iron-hydrogen mixing ratios at kT = 1 keV and P = 10^5 Mbar. I - pure hydrogen, II - 50% iron, III - 90% iron.

Fig. 2. Ratio of positive and negative charge densities in iron for various iron-hydrogen mixing ratios at kT = 1 keV and P = 10^5 Mbar. I - pure iron, II - 90% iron, III - 50% iron.

Fig. 3. Electron potentials for hydrogen in an iron-hydrogen mixture of x = .5, kT = keV, P = 10^5Mbar. I - DHTFD, II - CATFD.

Fig. 4. Same as Fig. 3 for iron.

Fig. 5. Electron potentials for hydrogen in an iron-hydrogen mixture of x = .3, kT = 10 eV, P = 10^2Mbar. I - DHTFD, II - CATFD.

Fig. 6. Same as Fig. 5 for iron.

Fig. 7. Change in the Gibbs potential due to mixing of iron and hydrogen. I - 1 keV, 10^5 Mbar; II - .8 keV 10^5 Mbar; III - .5 keV, 10^5 Mbar; ··· 1 keV 3×10^5 Mbar.

Fig. 8. Same as Fig. 7 at kT = 10 eV. I - 10^2 Mbar, II - 10 Mbar, III - 2 Mbar.

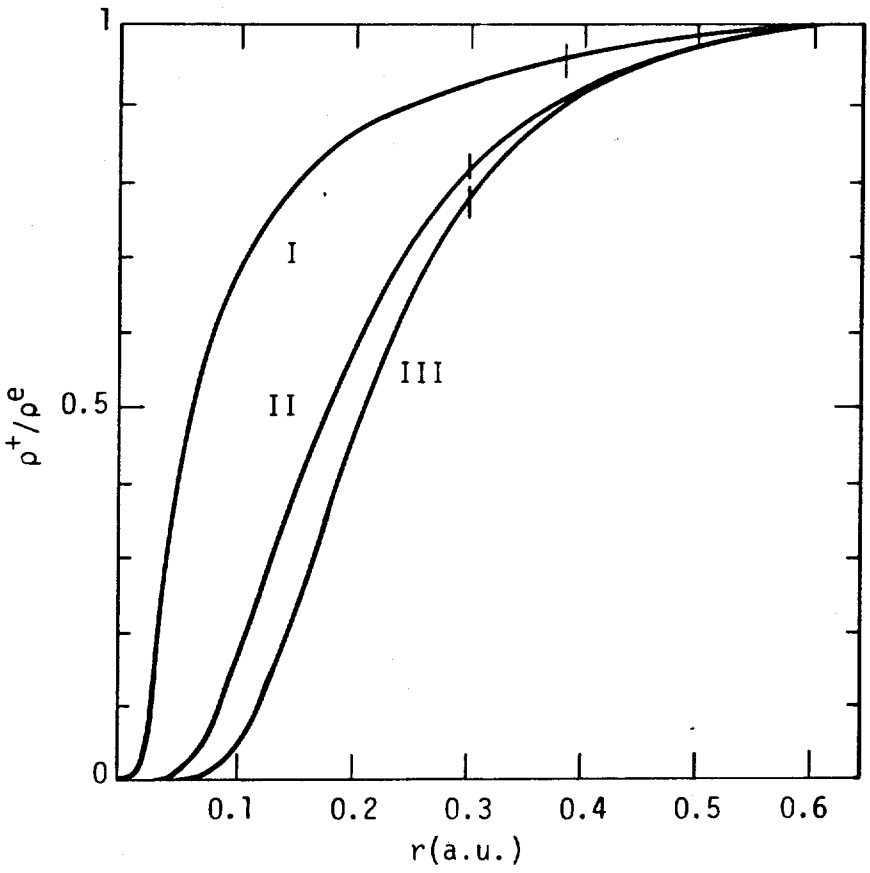

Fig. 1

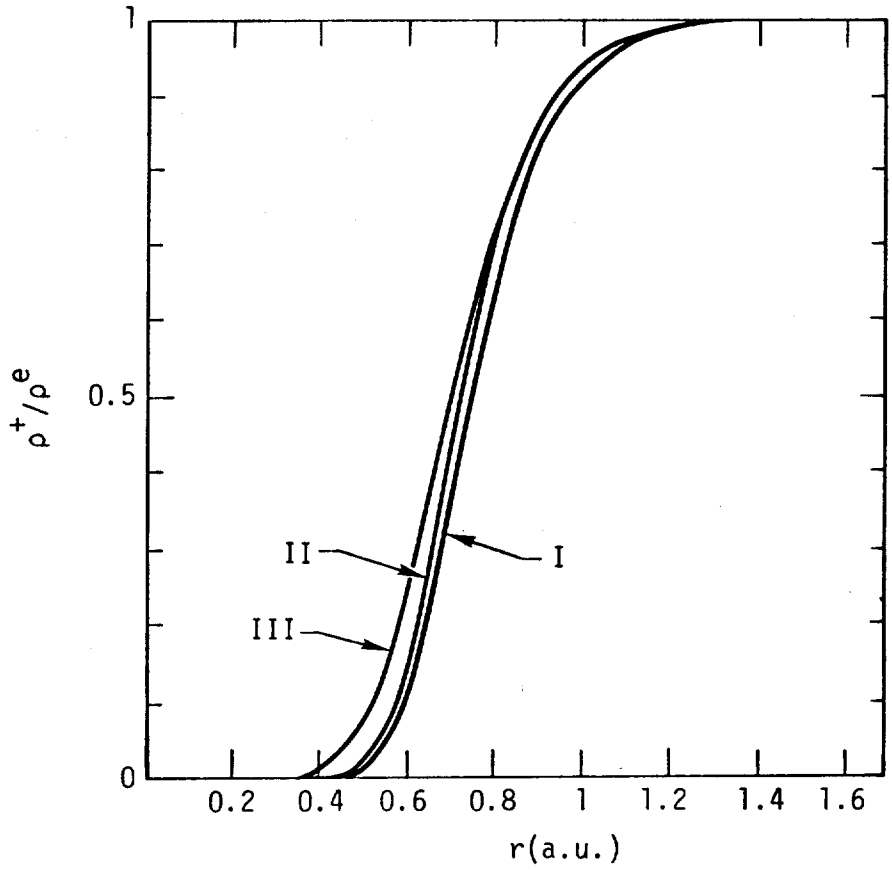

Fig. 2

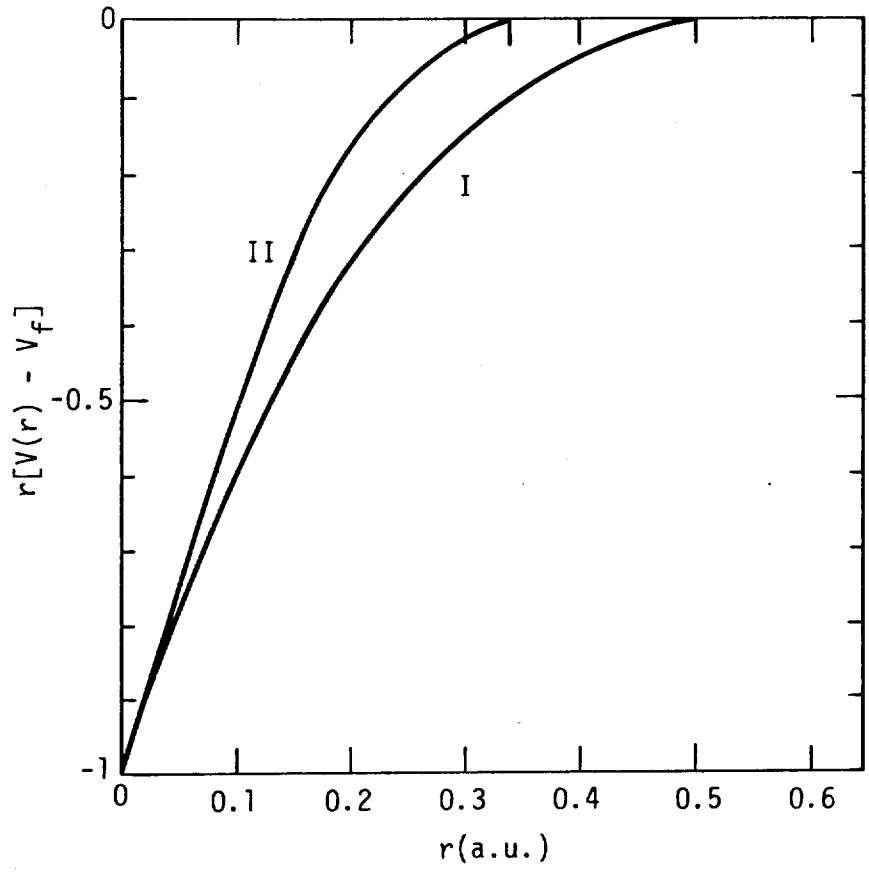

Fig. 3

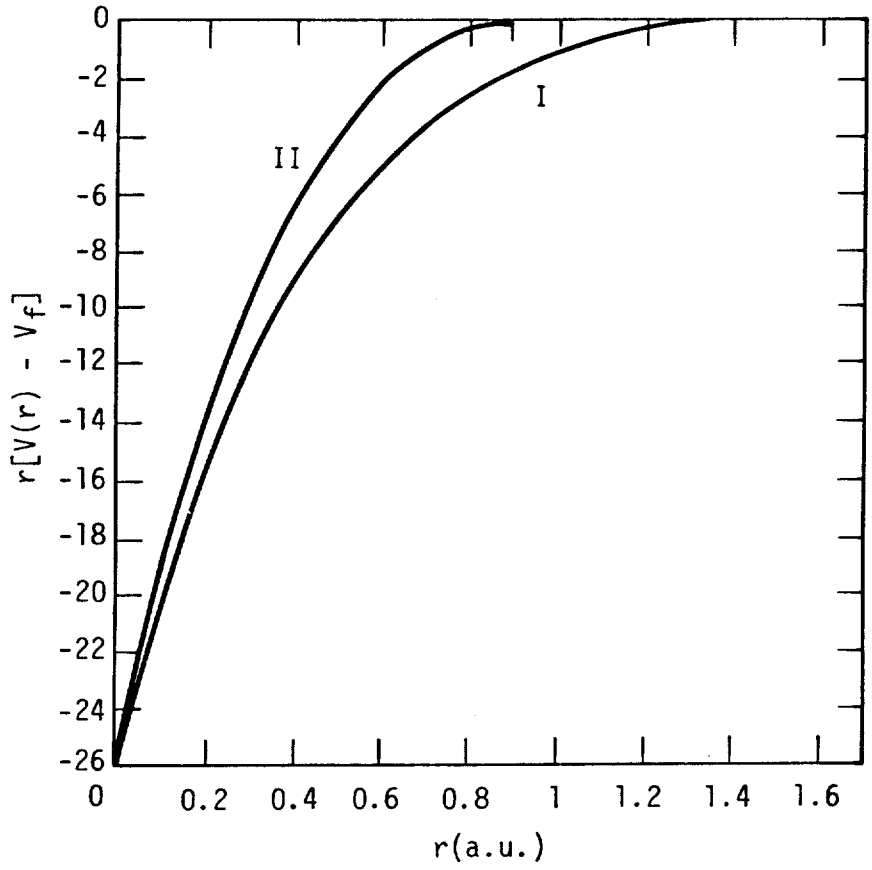
0
-2
-4
-6
-8
-10
-12
-14
-16
-18
-20
-22
-24
-26
r[V(r) - Vf]
0
0.2
0.4
0.6
0.8
1
1.2
1.4
1.6
r(a.u.)
I
II

Fig. 4

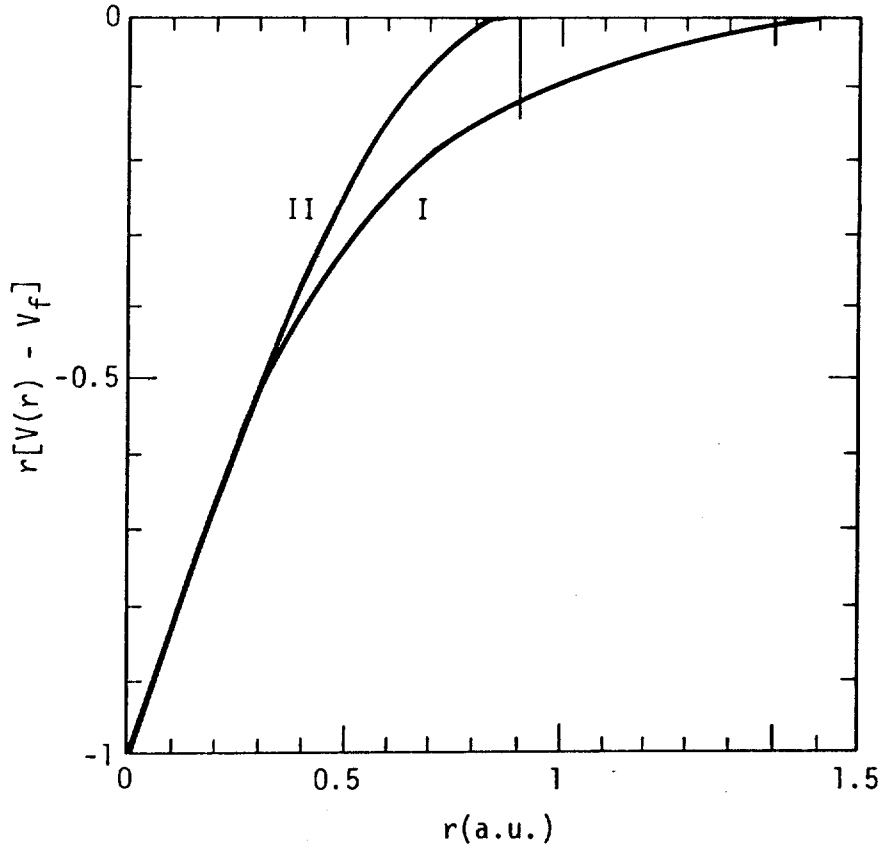

Fig. 5

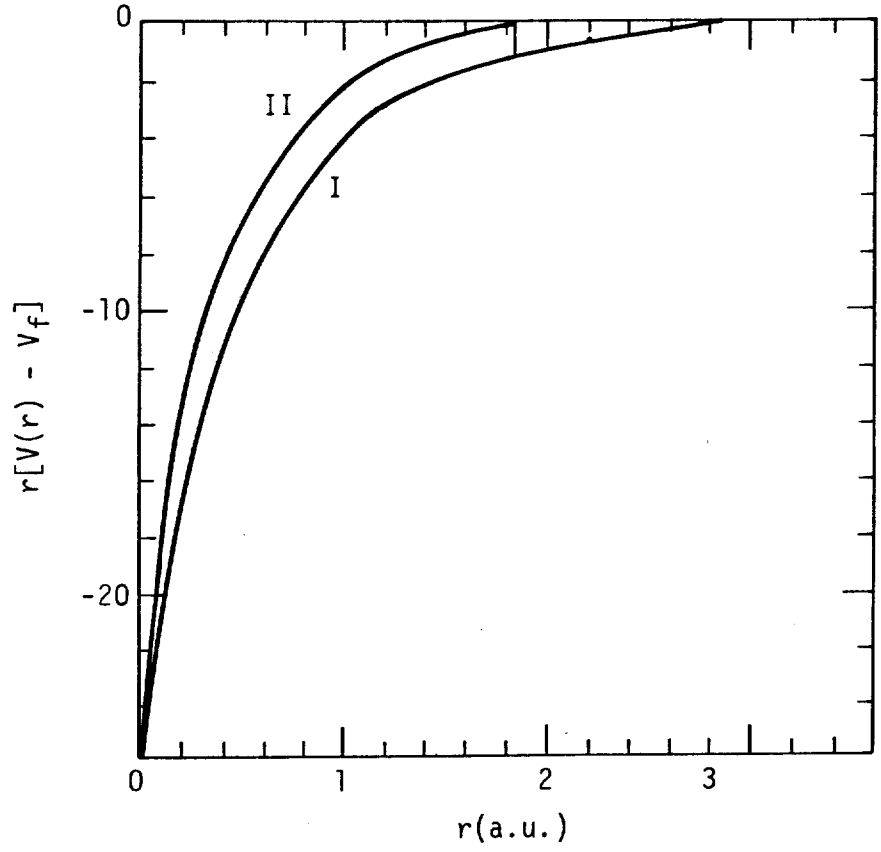

Fig. 6

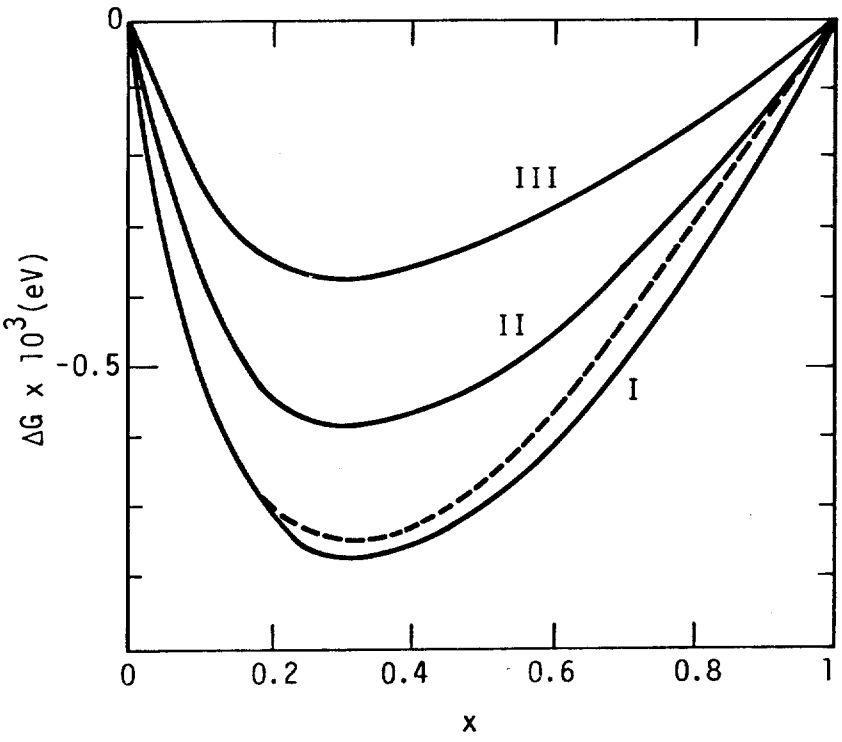

Fig. 7

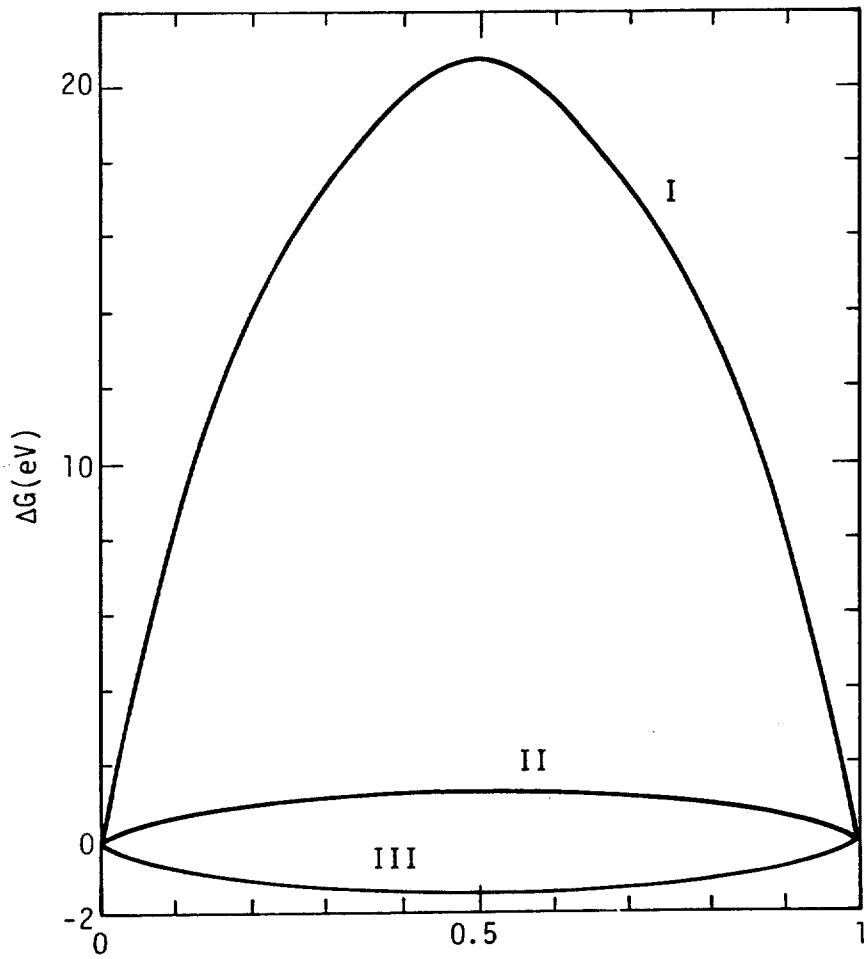

Fig. 8

Distribution

Balazs Rozsnyai	5
T.I.D.	15
T-Division File	3